PUMA EXPERIMENT

antiProton Unstable Matter Annihilation Project

Anthia Trakkoudi

Department or Physics
University of Cyprus(UCY)

Supervisor: Clara Klink, Francois Butin

Date: July, 2024

Abstract

The antiproton Unstable Matter Annihilation (PUMA) experiment aims to transport antiprotons from CERN's Antimatter Factory to the ISOLDE facility to research exotic nuclear phenomena. The general purpose is to determine the relative densities of protons and neutrons at the surface of these nuclei.

In this report, the commissioning of the trigger barrel is described. It is responsible for reconstructing the trajectories of the reaction products of the annihilation, mostly pions, in three dimensions. It was built, the electronics setup completed, the trigger logic configured and first data acquisition with cosmic radiation performed.

Contents

1 Introduction and Overview

The antiproton Unstable Matter Annihilation (PUMA) experiment aims at studying the nucleonic composition in the outer regions of the nuclear density distribution of both stable and exotic nuclei by using antimatter, and more specifically antiprotons.

This innovative concept was conceived by Alexandre Obertelli, with the aim to investigate potential exotic phenomena arising from low-energy interactions between antiprotons and slow-moving exotic nuclei. Hence, scientists must trap antimatter and transport it to a facility that generates radioactive ion beams. ELENA is a storage ring for antiprotons, where they can be decelerated to an energy of around 100 keV. The initial phase of the PUMA experiment will occur at ELENA before the antiprotons are transported to the ISOLDE facility for further study of exotic nuclei. From ELENA, antiprotons are transported to the PUMA experimental zone, where they are decelerated via the pulsed drift tube and then injected into the antiproton trap. Additionally, there is an offline ion source beamline that generates charged isotopes in an ion source. This beamline is responsible for mass-separation of the ions of interest and an accumulation of the ions in bunches.

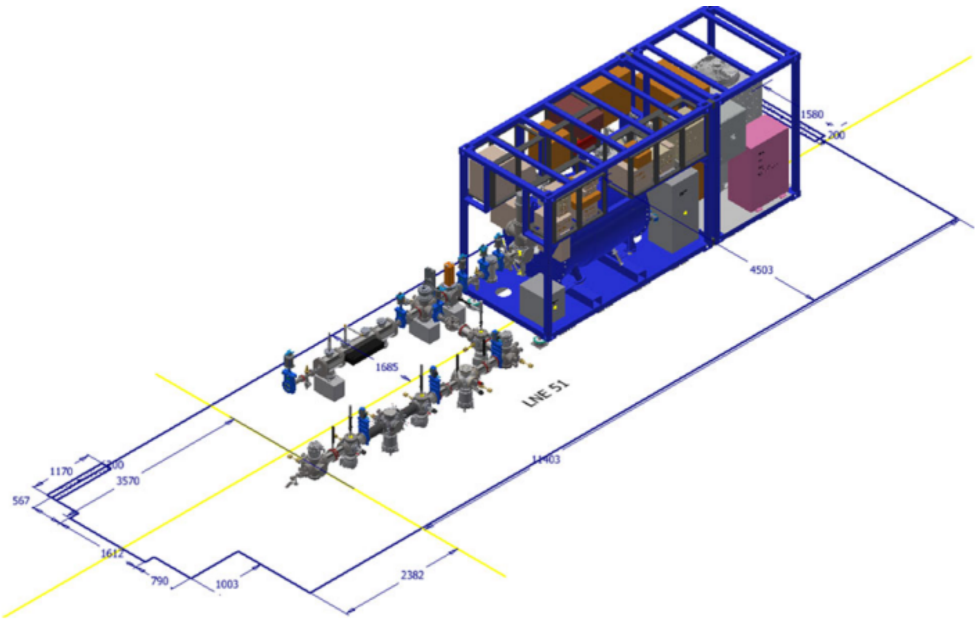

Figure 1: An overview of the PUMA setup, which consists of a magnet, a trap, a PUMA beamline, and an ion source beamline. [1]

Cosmic radiation consists of high-energy particles originating from outer space, including protons, atomic nuclei, and gamma rays, which can penetrate Earth's atmosphere and interact with atmospheric particles, creating secondary radiation. Low-energy terrestrial radiation, on the other hand, comes from naturally occurring radioactive materials within the Earth's crust, such as uranium, thorium, and radon. These emit lower-energy alpha, beta, and gamma radiation. Cosmic rays are Minimum Ionizing Particles (MIPs), and the pions we want to observe in this experiment are also MIPs. Therefore, if we can effectively detect cosmic rays, we will also be able to detect pions well. The Trigger Barrel is designed to identify and filter out these types of background radiation. By distinguishing between cosmic and terrestrial radiation events, it helps ensure that only relevant particle interactions are recorded for further analysis, enhancing the accuracy of experimental data in high-energy physics research.

A specially designed, dual-zoned trap, approximately 70 cm long and housed within a superconducting solenoid magnet, will ensure the antimatter cloud remains intact during its journey and can be stored for an extended period. The storage zone will maintain 1 billion antiprotons in a plasma, which are collected from ELENA, at a temperature of 4K.

In the first trap, antiprotons are stored. The second trap mixes these antiprotons with ions of interest produced either in the offline ion source beamline or with unstable atomic nuclei produced at ISOLDE.

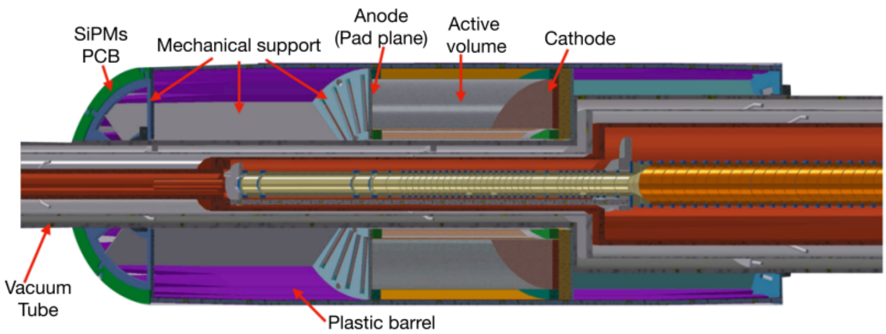

Figure 2: A cut view (half is shown) of the proposed setup CAD model and mechanical support of the detection system in the collision zone. It presents a sketched 3D view of the pion detection system for the collision zone. The TPC is a 300mm long cylinder, 53mm internal radius and 110mm external radius, filled with ionizing gas. [1]

By changing the trap potential, the antiproton plasma will overlap with the trapped ions. When a baryon, more specifically a proton which is a hadron composed of 3 quarks, collides with its anti-baryon, their quarks and anti-quarks annihilate which cause the production of mesons, more precisely pions which are hadrons composed of up and down quark and antiquarks.

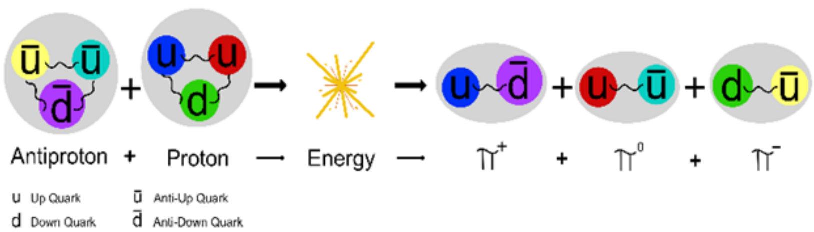

Figure 3: Annihilation of a proton and antiproton resulting in the production of pions.[2]

Due to conservation law of charge, this whole process must have zero total charge Q=0. Accordingly, an antiproton-neutron annihilation has Q = -1.

The particle detector identifies the charge of pions resulting from the annihilation between antiprotons and and surface nucleons in the interaction trap.

The pions which are produced by the proton and antiproton annihilation, travel on curved trajectories based on their charge since they are inside a magnetic field. By the curvature, one can identify the charge of the particle.

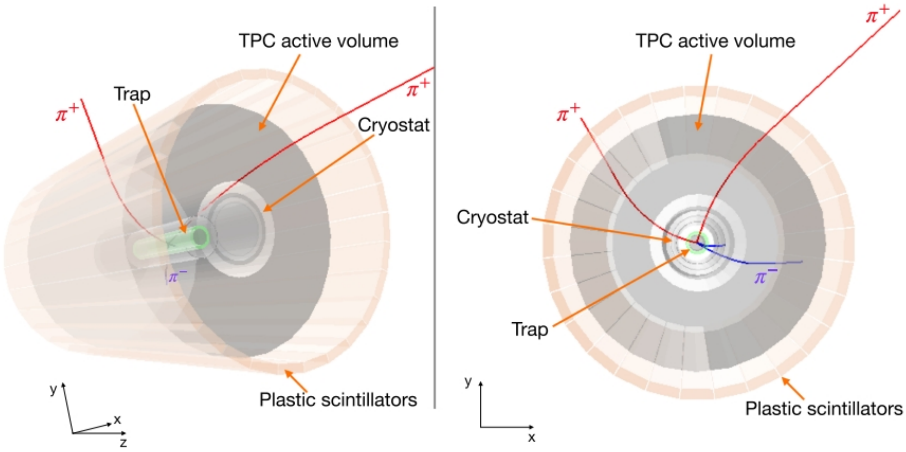

Figure 4: This figure presents a typical event in the collision trap surrounded by the TPC and the plastic barrel. The blue line corresponds to a π^- and the red ones to π^+. [1]

2 The PUMA detector

During this summer project, the detector is commissioned. The time projection chamber together with the trigger barrel are responsible for a full track reconstruction. The first-time operation of the full trigger barrel is the final goal of this project.

2.1 Time Projection Chamber(TPC)

This TPC works by combining electric and magnetic fields within a gas-filled chamber to reconstruct the trajectories of the pions in three dimensions. A TPC contains of a gas-filled volume where particles pass through and ionize the gas. An electric field is established within this chamber, usually between a central high-voltage electrode and the end plate. This field causes the electrons produced by the ionization of the gas to drift towards the end plate. The end plates are equipped with a position-sensitive electron collection system, such as multi-wire proportional chambers or pad readouts. This system detects the position of the incoming electrons. A magnetic field is often applied along the length of the chamber, parallel to the electric field. This field helps minimize the diffusion of electrons as they drift, leading to more precise tracking. By measuring the time, it takes for the electrons to drift to the end plates (time projection) and their position upon arrival, the TPC can reconstruct the three-dimensional path of the particle that ionized the gas. [3]

2.2 Function of Trigger Barrel

A general picture of the trigger barrel together with the TPC is shown in Fig. 4.

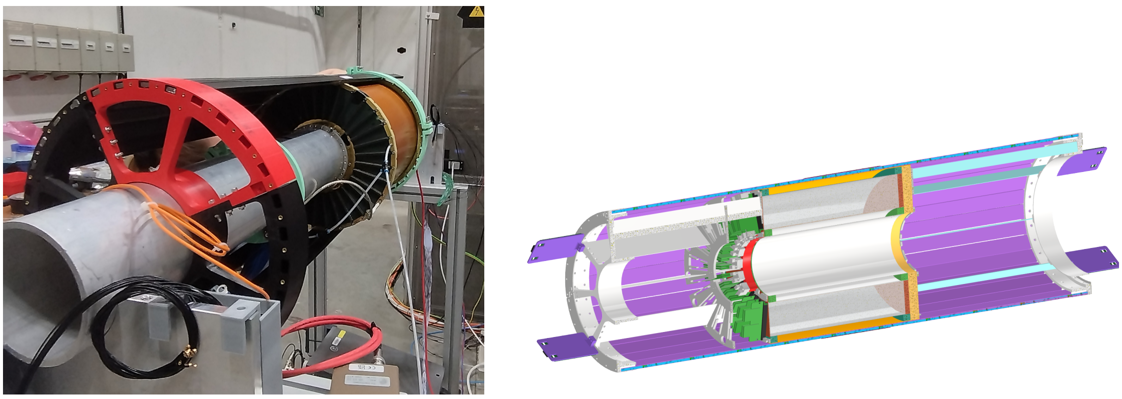

Figure 5: Trigger Barrel Mounted surrounding the TPC Inside.

Scintillation in general is a process where certain materials emit light (photons) when they are excited by ionizing radiation. This occurs when radiation like alpha particles, beta particles or gamma rays interact with the atoms or molecules of the scintillating material, causing them to become excited. This excited atoms or molecules then return to their ground state, releasing the excess energy as photons. The emitted light is detected by the silicon photo-multipliers which convert the light into electrical signals for analysis.

After a pion leaves the detection volume of the TPC radially, it passes through the surrounding trigger barrel. The trigger barrel consists of 32 cylindrically mounted scintillators. The light passes through the scintillators and then gets detected by the four silicon photomultipliers (SiPMs) which are connected to each side of the scintillators. Afterwards, these four signals are detected in coincidence by the TRB electronics and forwarded as a trigger to the time projection chamber. Furthermore, the trigger barrel allows to determine background and annihilation rates in the detector. Consequently, the amount of rest gas can be determined by observing the annihilation rate in the detector.

Through this process, pions, which are high-energy particles moving through space with minimal interactions, are able to fly faster than electron drift through the gas due to their respective mechanisms of motion and forces acting on them. Once produced, pions move with high kinetic energy and experience relatively few interactions compared to electrons in a gas, which are subject to frequent scattering wit gas atoms or molecules leading to a much lower average velocity (drift velocity). For this reason, we can use the resulting signal as a trigger for the TPC which subsequently gives access to the third dimension in the track reconstruction.

The trigger barrel scintillators are longer than the detection volume. This was planned so that they also enclose the storage zone, positioned opposite the detector. This arrangement was designed to identify any rest gas in the storage zone, ensuring that the background annihilation rate is minimized. Additionally, during the transport process, the setup will be able to tag antiprotonic losses. If for example all antiprotons annihilate at the same time because the trapping fields are lost and they collisde with the trap walls, a high annihilation rate will be observed with the trigger barrel.

3 Mounting Process

3.1 Barrel Mounting

Before beginning the mounting process, the wheels must be equipped with inlets and the squeeze rods inserted without hindering the plastics. As shown in the fig 6, the gold rods should be positioned under the scintillator pocket, where screws will be inserted to secure the scintillators in place.

Figure 6: Mounting wheel with inlets(gold) and screws(silver) to secure the scintillators inside the wheel pockets.

Next, the scintillators are mounted on the wheel, ensuring their tips are fully inserted into the pockets of the first wheel so that they lie flat. We secure the position by tightening the two screws below the pocket. Then, the second wheel is added. We make sure the wheels are aligned with the same rotation so that the power boards can be mirrored accurately.

Next, we apply the optical pads to the open sides of the plastics. We position the power boards on both sides so that the SiPMs touch the faces of the scintillators, securing each board with screws and connecting the concentrator boards for the PADIWA3 in a mirrored configuration.

3.2 Electronics Setup

All of the components used in this process are illustrated in Fig. 7.

Setting up an electronic system involves arranging and configuring various electronic components to perform specific functions or experiments. In this particular setup, a 5V low power supply is utilized for both the PADIWA modules and the TRB crate. An oscilloscope is employed to check the signal output from each scintillator. Lemo cables are used to provide power to the SiPMs, while ribbon cables are used to connect the PADIWA modules to the Time-to-Digital Converters (TDCs). The TDCs are mounted alongside the master module and the CTS within the TRB crate. The master module and the CTS are then connected to a computer via a network switch for data communication and control.

Initially, we connect the SiPM power supply to all eight power boards using Lemo cables, which are designed for low voltage power distribution. These power boards are connected to a low voltage (LV) power supply.

Next, the concentrator boards, ribbon cables, and power cables are connected. The PADIWA modules on opposite sides of the setup are connected to the same TDC on DAC chain 0 and 1 using ribbon cables. The power cables for the PADIWA modules are connected to a 5V low power board, which is itself powered by one of the LV power supplies.

This configuration ensures that each component is properly powered and interconnected, allowing for the efficient collection and analysis of data. The comprehensive details of the setup process and the function of each component are thoroughly explained in the manual, ensuring that users can accurately replicate the setup for their specific experimental needs. [4]

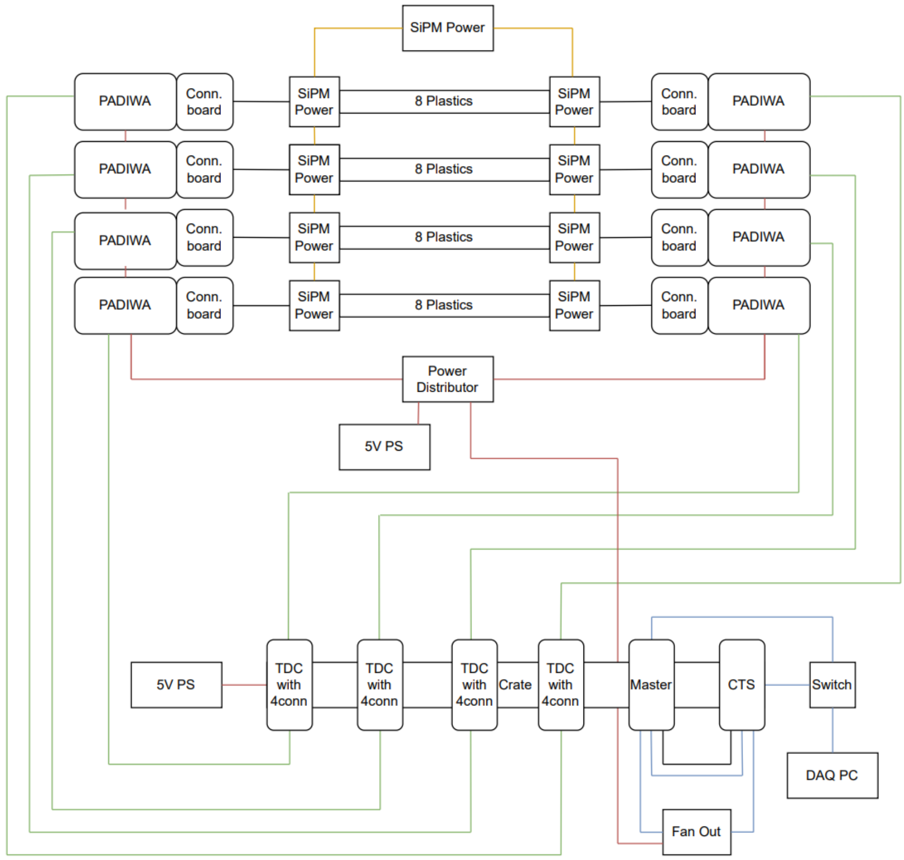

Figure 7: This is a diagram of the complete electronics setup. It illustrates a data aqcuisition system which involves Silicon Photomultipliers (SiPMs) which are optically connected to plastic scintillators. Each SiPM power module is connected to 8 connected plastic scintillators and interfaces with PADIWA preamplifier boards through connector boards. Power is managed by a central Power Distributor, which receives input from a 5V low power suplly and distributes it to the SiPM Power modules and TDCs. The TDCs are connected to 2 PADIWAs each and are responsible for precise event timing and are powered by a separate 5V low power supply. The TDCs feed data to a Master unit and a CTS (Central Timing System) which synchronize and control the system. A fan out component forwards the trigger signal to the TPC, while a switch connects the system to a DAQ PC for data collection and analysis.[4]

Ensuring light protection is crucial for the proper functioning of the trigger barrel system. This aspect needs to be carefully assessed and incorporated into the design of the final mounting setup. At present, a specialized dark tape is employed in the current, non-optimized assembly process, but it is essential to address and cover the rear sides of the power boards and seal all gaps thoroughly to prevent light interference.

By interfacing with the system through a computer, we can verify the number of boards connected to the PADIWAS system. This allows us to retrieve and review each board's identification by its serial number. Additionally, the system enables us to monitor the temperature and operational rates of each channel on the boards, ensuring their performance is within the expected parameters.

3.3 Trigger Setup

The main goal of this process is to organize four channels into a channel group according to the configuration of the scintillators. Each PADIWA module connects to four scintillators and comprises 16 channels, with each scintillator linked to four channels, two on each side. For example, the first two channels of PADIWA 1 connect to one side of a scintillator, while the first two channels of PADIWA 2 connect to the other side. An event is considered only when signals are received by all four channels, ensuring effective noise suppression in the data. [4]

To configure the trigger, we use the Input Monitor and Trigger Logic accessible via the web interface. This interface allows to select channels of interest and apply different trigger logic configurations to them.

When the trigger monitor identifies a combination of channels that fulfil the predetermined trigger logic within a given coincidence time window, the event is saved.

In this configuration, channels 1 and 2 of PADIWA 1 correspond to TDC channels 1 and 2, while channels 1 and 2 of PADIWA 2 correspond to TDC channels 17 and 18. Thus, each scintillator is associated with a group of four channels in a similar manner.

Only the multiplicity coincidence can be used to group channels this way, as the trigger should only activate when all four channels detect a signal.

[**einstein**] [**Aumann:2811200**]

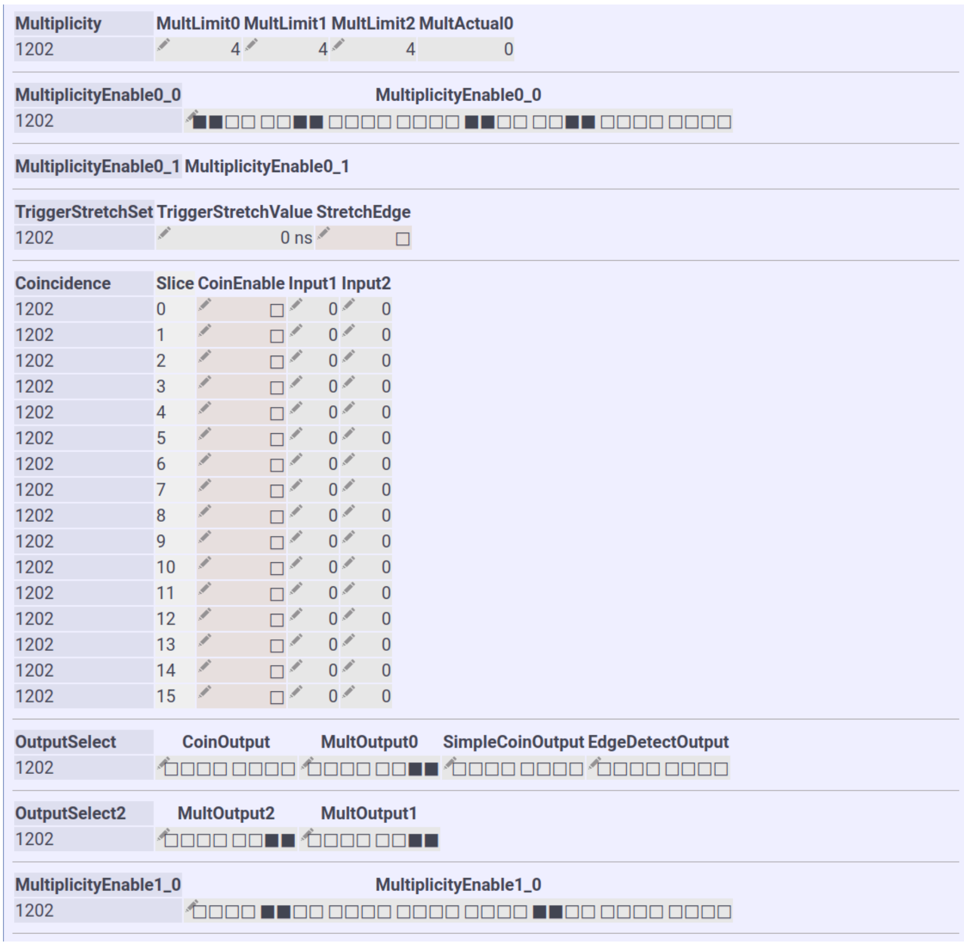

Figure 8: This is an overview of the Trigger Setup coincidence feature accessible through the web interface. By utilizing the multiplicity coincidence function, we can configure specific channel groupings by selecting the appropriate checkboxes.

To convert binary numbers into the boxes illustrated in Fig. 7, we start by counting the binary digits from right to left. Each box in the figure represents a single binary digit (bit), with a black box indicating a '1' and a white box indicating a '0'. This visual representation helps in quickly identifying the binary values.

For instance, to select the 7th and 8th channels, we count the positions from the rightmost box to the left. The 7th and 8th boxes are highlighted as black, representing the binary number 1100 0000. This binary sequence is then segmented into groups of four digits (bits) for easier conversion into hexadecimal form, which is more compact and manageable for data entry. The binary sequence 1100 0000 translates into the hexadecimal number C0, where '1100' is 'C' and '0000' remains '0'.

This conversion process is crucial for accurately setting configurations and ensuring the correct channels are selected. By converting binary to hexadecimal, we simplify the process of inputting these configurations into the system. This method is particularly useful in digital systems where precise channel selection and configuration are necessary for proper operation and data analysis.

4 Measurement

4.1 Data Aquisition

In order to collect our data, we initiate the process by connecting to our web server, which is accessible at localhost:8091. Once connected, we check the monitoring box within the interface. In the EventCombiner section, we proceed by opening the startFile option, give a name to our data file, and then click the execute button to begin data collection. In the HadaqCombiner, the number of recorded events can be observed in live-time. In stopFile, we terminate the data aquisition process. This sequence of actions ensures that our data file is successfully recorded and saved as an hld file, a data stream file format, to our computer.

The next step is to transform this hld file into a ROOT file by giving the following commands:

- export CALMODE = 0
- go4analysis -user DataFile.hld
- root unpackdData.root

4.2 SiPM signal shape

To observe the signals generated by one scintillator, an oscilloscope was employed to capture and display the waveform characteristics of the cosmic radiation. At first, as seen from the Fig. 9, we observe a rapid rise due to the quick collection of the primary charge carriers, followed by a decay. This decay corresponds to the slower process of charge carriers drifting to the electrodes. The width of each pulse is quite narrow in the range of 200ns. For each channel, we have different baselines with background noise. However, the noise has usually a lower amplitude compared to the pulses from actual radiation events we receive. The area under the signal curve is proportional to the energy loss of the charged particle in the scintillator.

By setting a threshold, we are able to define a minimum signal level that must be reached for the oscilloscope to recognize and record a pulse as a valid radiation event. This method helps us improve the signal-to-noise ratio, as it ensures that only genuine radiation events are detected, reducing the likelihood of false positives caused by noise. Also, by ignoring pulses below the threshold, the amount of data collected and processed is reduced. Hence, this makes data analysis more manageable and efficient.

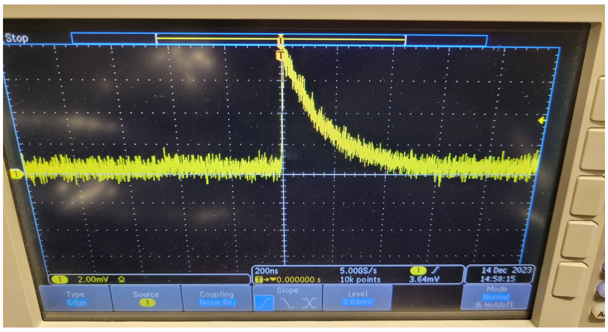

Figure 9: Signal shown on the oscilloscope from one SiPM.

4.3 Time Over Threshold

In Fig.10 an example signal is shown. By setting a specific threshold(red line) on a signal, we can measure the 'time over threshold', which is the time interval between when the signal first exceeds (rising point - t1) the threshold and when it falls back below it (falling point - t2). This interval corresponds to the duration of the detectable signal (dt = t2 - t1).

The area under the signal curve during this time interval represents the energy lost by the particle in the material.

$$A \propto E$$

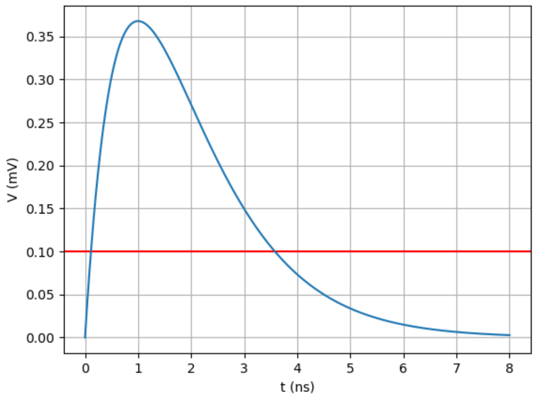

Figure 10: A graph illustrating a SiPM signal. We select a specific threshold (red line) to filter out noise signals, which have lower voltage amplitudes compared to the electrical signals received from the scintillators.

Since the area under the curve is proportional to the time over threshold, a longer time over threshold indicates a larger area and therefore greater energy loss.

$$dt \propto E$$

The signals can be evaluated in ToT histograms, considering different threshold levels. The threshold levels are given in arbitrary units and refer to the difference to the baseline to each channel. Eight scintillators were mounted in a dark room to avoid as much light contamination as possible. The following thresholds were considered: 0x1c0 and 0x400. We then used optical pads on all scintillators for the best optical performance. The red and black signals were collected from one side of the scintillators, while the green and blue signals were collected from the opposite side. Additionally, different voltages were applied to the scintillators to optimize their performance, specifically 26.2 V, 27.2 V, and 28.7 V.

4.4 Results

A histogram of the ToT for cosmic radiation for a threshold of 0x1c0 is shown in Fig. 11 display the histogram of 'Time over Threshold' measurements for the 8 scintillators.

The x-axis was divided into bins of 10-point intervals ranging from 0 to 100. Each bin represents a time difference value of our threshold (dt = t2 - t1).

The y-axis displays the counts of signals which have a specific time difference. Each histogram shows the frequency of occurrences of different time over threshold values dt, providing insights into the performance and characteristics of each scintillator.

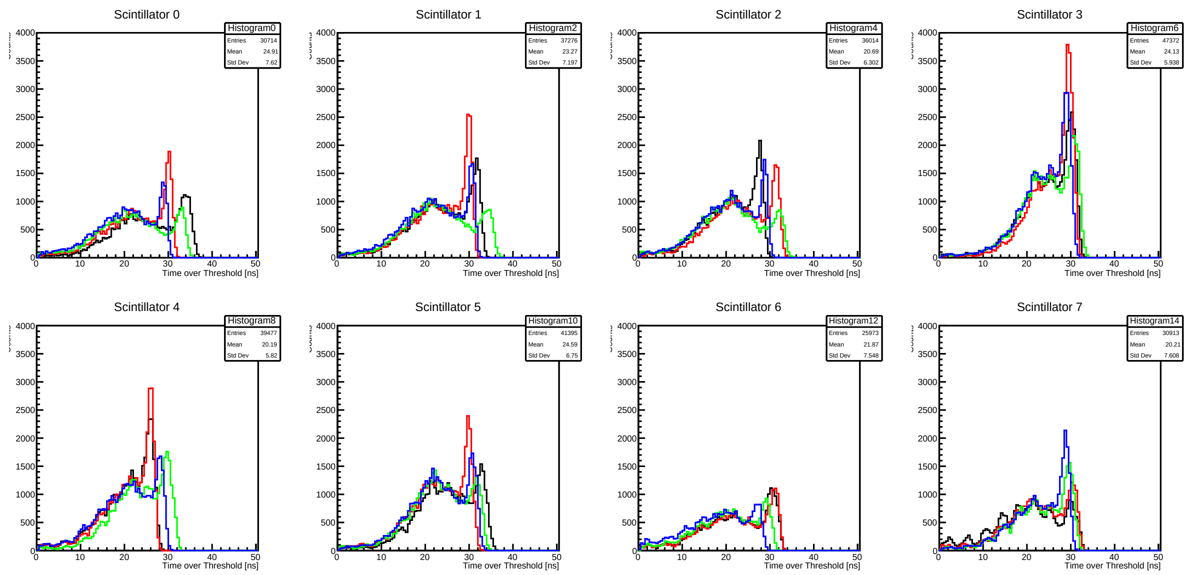

Figure 11: A histogram showing the counts of events per time difference of a 0x1c0 threshold at 27.7V. There are 4 channels per scintillator histogram. Red and black corresponds to the 2 SiPMs on the first side, blue and green to the 2 SiPMs on the other side.

From the graphs presented in Fig. 11, it is evident that a broad second peak appears to the left of the MIP peak in all scintillators. These are low-energy terrestrial background signals, that are cut at higher threshold levels.

From the scintillators 3 and 4, we notice a higher peak, which is expected since these scintillators are positioned in an almost horizontal position, and the other are more tilted around the detector, allowing them to receive more cosmic radiation and resulting in a higher detection rate.

However, it can be observed that the peaks in these histograms are not precisely aligned, indicating a constant shift. This inconsistency could be because the optical connection is not optimal or because the voltage would have to be tuned for each SiPM, which is not possible in our case since all SiPMs share the same voltage supply. Additionally, the detection electronics can cause slight delays, leading to the observed misalignment in the signals. The same issue occurs with scintillators 0 and 1, as the signals of each channel are not aligned with each other. This can be calibrated at a later stage with data.

Sometimes, the two sides are misaligned, indicating that the optical pads are not fully covering the SiPMs, leading to small gaps between the materials and resulting in incomplete signal reception.

The same histograms were constructed for the 0x400 threshold, as shown in Fig. 12, displaying the same distribution for the 8 scintillators.

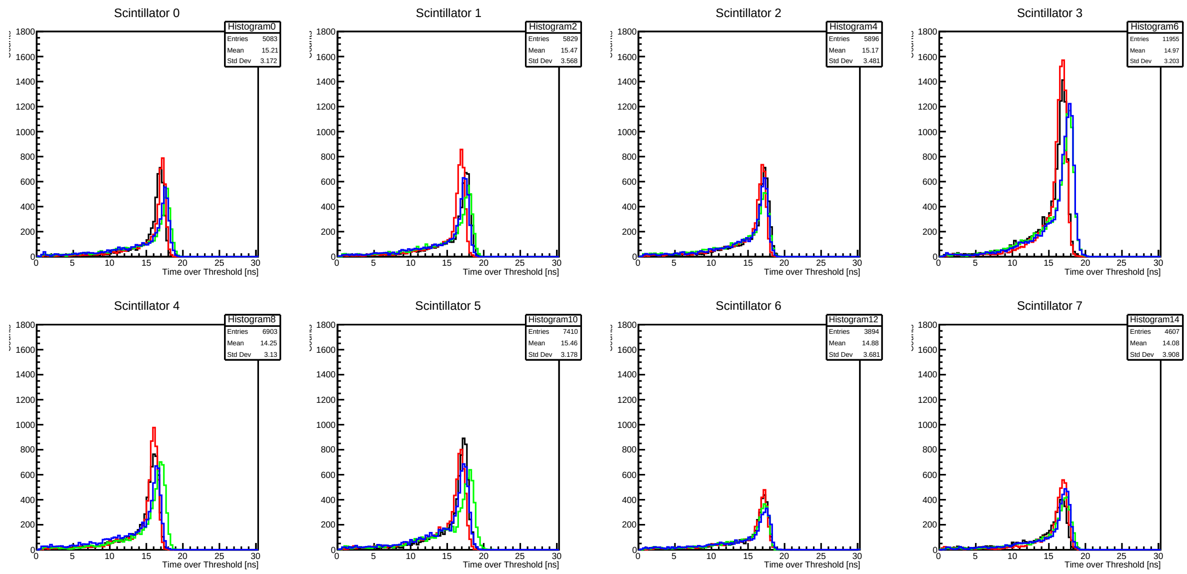

Figure 12: A histogram showing the counts of events per time difference of the threshold of a 0x400 threshold at 27.7V.

The results from the graphs presented in Fig. 12 demonstrate that by applying a higher threshold, the second peak on the left side is effectively eliminated. This indicates that the higher threshold successfully filters out low-energy terrestrial background signals, allowing us to isolate and receive only the desired signals from cosmic radiation that passes through the scintillators. This enhancement in signal clarity is of advantage for detecting minimum ionizing particles.

Now, with the threshold held constant at 0x400, we shift our focus to varying the voltage to study its impact on the signal detection. We took measurements using voltages of 26.2 V, 27.2 V, and 28.7 V to observe how these changes influence the performance and sensitivity of the scintillators.

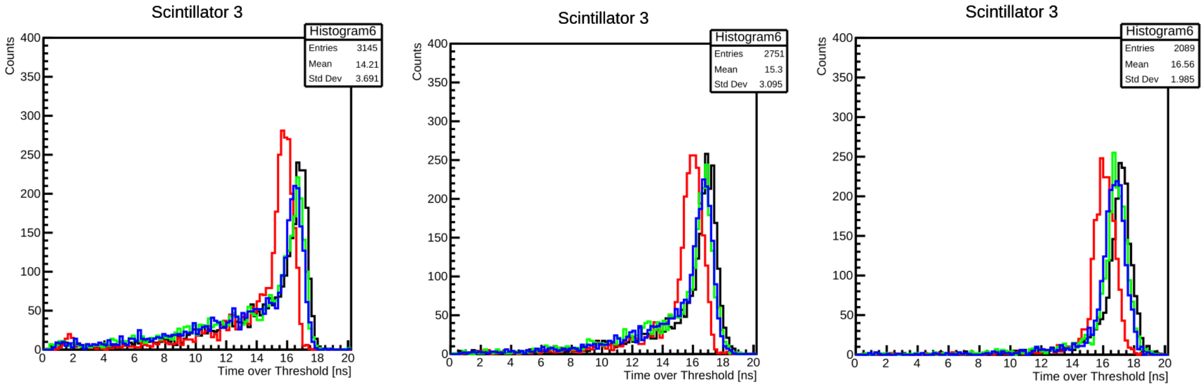

(a) 26.2 V (b) 27.2 V (c) 28.7 V

Figure 13: Three histograms showing the events per time difference of a 0x400 threshold with different voltage values on scinitllator 3.

From the graphs presented in Fig.13, it is evident that by increasing the voltage the tail on the left side of the peak decreases. That is because by increasing the voltage applied to the scintillator 3, it enhances signal amplification. Higher voltage improves the efficiency of converting photons into electrons. This results in a more effective conversion of incoming photons into detectable electrical signals. Consequently, the electrical signals become clearer and more distinct, minimizing incomplete or noisy data. Additionally, the fluctuations in the number of electrons generated per photon are reduced, as the voltage ensures a more consistent conversion rate, leading to fewer variations and more stable measurements.

5 Conclusions

In this project, we focused on planning and advancing the commissioning of the PUMA detector for the PUMA experiment. The primary focus was the installation of the trigger barrel and the integration of the time projection chamber(TPC).

From our results, we were able to receive signals from all the channels and scintillators from cosmic radiation and filter terrestrial low-energy background. However, we need to improve the optical connection between the scintillators and the SiPMs before continuing to install the rest of the barrel.

References

[1] T Aumann et al. "PUMA, antiProton unstable matter annihilation". In: *Eur. Phys. J. A* 58.5 (2022), p. 88. DOI: `10.1140/epja/s10050-022-00713-x`. URL: `https://cds.cern.ch/record/2811200`.

[2] Alpha Collaboration. *Annihilation Detectors*. `https://alpha.web.cern.ch/science/annihilation-detectors`. Accessed: 2024-07-31. 2024.

[3] Alexandre Obertelli. "Experiment Proposal for PUMA: antiprotons and radioactive nuclei". In: *CERN-SPSC-2019-033 / SPSC-P-361* (Sept. 2019), p. 177.

[4] Clara Klink Christina Xanthopoulou. "Electronics User Guide". In: (June 2024), p. 25.